Vietnam Journal of Earth Sciences, 48(2), 192–207, https://doi.org/10.15625/2615-9783/23990

Vietnam Journal of Earth Sciences
https://vjs.ac.vn/index.php/jse

Experimental evaluation of a single geogrid-reinforced stone column under varying surrounding soil conditions: Effects on bearing capacity and elastic modulus

Nguyen Thai Linh[1], Nguyen Hai Ha[1*], Nguyen Duc Manh[1], Indra Prakash[2], Vu Anh Tuan[3]

[1]*University of Transport and Communications, Hanoi, Vietnam*
[2]*DDG (R) Geological Survey of India, Gandhinagar 382010, India*
[3]*Geotechnical and Artificial Intelligence research group (GEOAI), University of Transport Technology, Hanoi, Vietnam*

Received 29 October 2025; Received in revised form 12 December 2025; Accepted 22 December 2025

ABSTRACT

This experimental study evaluates the influence of soil consistency on the ultimate bearing capacity and elastic modulus of single geogrid-reinforced and unreinforced stone columns installed in soft-to-very soft clay. Laboratory model tests were conducted in the Ho Thuong Tin area of Hanoi, Vietnam, under three controlled soil conditions with liquidity indices (IL) of 0.78, 1.0, and 1.5. A total of six displacement-controlled load tests were performed in a unit-cell setup, with and without a geogrid reinforcement layer at the column head. Results show that the inclusion of geogrid significantly enhanced both the ultimate bearing capacity and stiffness of the stone column: the bearing capacity increased by approximately 12–25%, and the elastic modulus (E_{50}) increased by 19–27% relative to unreinforced columns. The study indicates that geogrid reinforcement at the column head provides a technically material-saving and straightforward alternative to complete encasement, with potential economic advantages particularly for soft clays where lateral confinement is limited. The findings provide new experimental data to inform the design of geogrid-reinforced stone columns under varying soil conditions.

Keywords: Stone column, geogrid reinforcement, elastic modulus, load test, bearing capacity, laboratory model, soft clay, soil consistency.

1. Introduction

Stone columns, also known as granular columns or aggregate piers, are widely used in geotechnical engineering to improve the load-bearing capacity and settlement characteristics of soft or compressible soils. The principle is that the stiffer, more permeable stone columns act as drainage and reinforcement paths, thereby increasing overall stiffness, accelerating consolidation, reducing settlement, and enhancing bearing capacity (Barksdale et al., 1983). Stone column techniques have been applied to numerous geotechnical projects aiming to stabilize weak soils underlying embankments, roadways, foundations, storage tanks, and retaining structures (Singh and Sahu, 2019). Field assessments have confirmed that stone columns reduce both total and differential settlements and increase bearing capacity (McCabe et al., 2009).

*Corresponding author, Email: haihadkt@utc.edu.vn

In soft soils, installing a stone column enhances both load-bearing capacity and stiffness while reducing consolidation settlement. Many researchers have explored different facets of stone column technology. Their investigations have included evaluating the performance of a stone column in various soil conditions, such as in clay samples (Bergado et al., 1990; Black et al., 2007a; Hasan and Samadhiya, 2016; Miranda and Da Costa, 2016), soft clay foundations, layered soils, and sand stabilized with single or multiple geocells. Additionally, numerical analyses of the stone column's behavior have been conducted. (Hasan and Samadhiya, 2016; Muzammil et al., 2018). The lack of adequate lateral support in soft soils can significantly diminish the performance of a stone column, with this deficiency being most acute at shallow depths and often resulting in bulging failure in the upper portion of the column.

One of the key engineering parameters for evaluating the mechanical properties of stone column systems is the elastic modulus (E) of the column. The elastic modulus is the ratio of the normal stress to the corresponding strain within the material's elastic range. It is a fundamental parameter that reflects the material's stiffness and plays a crucial role in modeling and analyzing the deformation behavior of both the foundation soil and reinforcement elements, such as stone columns (Fatahi et al., 2012). The determination of the elastic modulus can be carried out using various experimental testing methods and numerical back-analysis methods. In addition to traditional laboratory testing and finite element simulations, recent advances in machine learning techniques have enabled more rapid and efficient prediction of foundation performance parameters, including the bearing capacity of deep foundations such as bored piles, based on limited in-situ and design characteristics (Pham et al., 2022).

The application of elastic modulus (E) in soft ground improvement is diverse, including settlement prediction, stress distribution analysis, reinforcement design, and evaluation of ground improvement efficiency (Dash and Bora, 2013; Fatahi et al., 2012; Fattah et al., 2017). A higher E value indicates more minor deformation under loading, thereby minimizing settlement and extending the service life of structures. Notably, in stone column systems reinforced with geosynthetics, the modulus of elasticity enables accurate simulation of elastic response and load transfer mechanisms, supporting optimization of design parameters such as column length, diameter, and geogrid placement (Kahyaoğlu and Doğan, 2022).

The determination of elastic modulus can be carried out through experimental testing and numerical simulation. The Plate Load Test (PLT) is a commonly used field technique that directly measures E by observing the load-settlement response. In addition, finite element method (FEM) analyses, often combined with the Hardening Soil model, are used to back-calculate E from experimental data, thereby improving design accuracy and predicting ground improvement performance. Triaxial compression tests and small-scale physical modeling have also been employed to determine the modulus under more controlled loading and boundary conditions.

Several experimental and numerical studies have been conducted to investigate the deformation characteristics of single stone columns and to estimate their elastic moduli for design and settlement prediction purposes. Yoo and Lee (2012) examined the performance of geosynthetic-encased stone column (GESC) in soft soils through full-scale load tests, demonstrating that geogrid encasement enhances lateral confinement, increases stiffness, and reduces settlement (Yoo and Lee, 2012). The effectiveness,

however, depends on the length of the encasement and the degree of column deformation. Cheng et al (2023) applied the finite difference method (FLAC3D) to simulate the behavior of floating ordinary stone column (F-OSC) and floating encased stone column (F-ESC), analyzing the influence of column length and encasement length on settlement, bulging, failure mechanisms, and load transfer efficiency (Cheng et al., 2023). Ling et al. (2020) carried out experimental studies on the cyclic loading behavior of foundations reinforced with geotextile-encased stone columns (Ling et al., 2020).

In addition, numerous numerical simulations have been used to back-calculate the elastic modulus (E) of stone columns from load-settlement curves, providing valuable data for the design of stone column foundations in soft soils. The findings collectively indicate that the elastic modulus of a single stone column is governed not only by the type and compaction of column material but also significantly by the geotechnical properties of the surrounding soil and the geometric configuration of the column. Reported values of E typically range from 20 MPa to more than 60 MPa, depending on test conditions and material characteristics. Overall, previous studies have highlighted the role of elastic modulus as an essential parameter for accurately modeling the mechanical behavior of stone columns and for improving the design efficiency of ground treatment through localized reinforcement.

Despite promising outcomes reported for enhancing load-carrying capacity and controlling settlement in stone column-reinforced foundations, most existing studies on geosynthetic reinforcement have focused on fully encased stone columns. Recent experimental and numerical investigations on geosynthetic-encased stone columns (GESCs) have demonstrated substantial gains in stiffness, reduced bulging, and improved load transfer, but they typically adopt full or long encasement configurations and seldom isolate the effect of local reinforcement at the column head. Head reinforcement using a single geogrid layer is technically simpler and reduces the amount of geosynthetic material, suggesting potential economic and construction advantages in cases where complete encasement is impractical due to installation constraints or cost.

To address this research gap, the present study conducts a systematic experimental investigation of single geogrid-reinforced stone columns with and without a geogrid layer at the column head, installed in soft clay under varying soil consistencies. Laboratory model tests were conducted using the unit cell approach on soft clay samples collected from the Ho Thuong Tin area, Hanoi, Vietnam, with liquidity indices ranging from 0.78 to 1.50. The primary objectives are to: (i) evaluate the influence of soil consistency on the ultimate bearing capacity and elastic modulus (E_{50}) of stone columns; (ii) quantify the improvement due to geogrid reinforcement at the column head; and (iii) compare the experimental outcomes with existing empirical and theoretical correlations. The results provide new experimental evidence and practical insights into the behavior of geogrid-reinforced stone columns under varying surrounding soil conditions, supporting the optimization of head-reinforced systems as an efficient and cost-effective solution for soft ground improvement particularly relevant to infrastructure development across Southeast Asia and similar geotechnical settings worldwide.

2. Methodology

The experimental program was designed to investigate the influence of soil consistency

on the ultimate bearing capacity and elastic modulus (E_{50}) of single stone columns with and without geogrid reinforcement. Laboratory model tests were conducted using the unit-cell approach, which simulates a single column surrounded by an equivalent volume of soft soil. The tests were performed under displacement-controlled loading conditions to simulate the column-soil system's response.

Three soft clay conditions were prepared by varying the moisture content to achieve liquidity indices (IL) of 0.78, 1.0, and 1.5. For each soil condition, two test configurations were examined:

Unreinforced stone column, and Geogrid-reinforced stone column, where a geogrid layer was installed at the column head.

A total of six tests were carried out. The main objectives were to determine the variation of bearing capacity, load-settlement characteristics, and the elastic modulus of the stone columns with respect to soil consistency.

2.1. Elastic modulus (E)

Elastic modulus (E) is a fundamental parameter characterizing the stiffness of soils and granular materials and is widely used in settlement analyses and numerical modelling of ground improvement systems. For stone column-reinforced ground, both the initial modulus (E_0) and the secant modulus at 50% of the ultimate load (E_{50}) are commonly employed to describe the stress-strain response under working loads and near-failure conditions.

In this study, the elastic modulus of the stone column at 50% of the ultimate load is determined from the load-settlement curves according to:

$$E_{50} = \sigma_{50}/\varepsilon_{50} \quad (1)$$

Where σ_{50} is the normal stress corresponding to 50% of the ultimate load; and ε_{50} is the axial strain of the column at this stress level. The definition of E_{50} follows typical practice in foundation engineering and is consistent with previous experimental and numerical studies on stone columns and soft ground improvement. A schematic stress-strain curve illustrating E_0 and E_{50} is shown in Fig. 1.

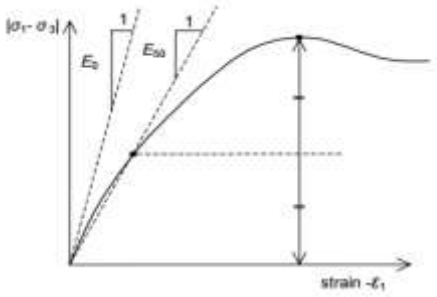

Figure 1. Stress-strain behavior of soil

2.2. Stone columns and the theoretical calculation of stone columns utilizing the elastic modulus (E)

The design of and analysis of stone column-reinforced ground are often based on inclusion theory and composite ground concepts, in which a representative unit cell comprising one column and the surrounding soil is considered. Under vertical loading, the stone column and the soil deform compatibly in the vertical direction, and the stress distribution between the two materials depends on their relative stiffness and the area replacement ratio.

A key parameter in simplified settlement analyses is the stress concentration ratio n, which relates the average stress in the column to that in the surrounding soil. Based on the empirical chart by Barksdale et al. (1983), Han and Ye (2001) proposed the following expression:

$$n = 1 + 0.217\left(\frac{E_c}{E_s} - 1\right) \quad (2)$$

where in: n is the stress concentration ratio; E_c and E_s are the elastic modulus of the column and the soil, respectively.

The corresponding stress reduction factor

μ, expressing the proportion of the applied stress carried by the reinforced ground compared to untreated soil, is given by:

$$\mu = \frac{1}{1+(n-1)a_s} \quad (3)$$

Where a_s is the area replacement ratio. The post-treatment settlement S′ can then be approximated as:

$$S' = \mu S \quad (4)$$

where S is the settlement of the untreated ground.

An alternative but equivalent approach is to model the reinforced ground as a two-phase composite with an equivalent elastic modulus E_{eq}, obtained by a weighted average of the soil and column moduli over the unit cell area (Barksdale et al., 1983):

$$E_{eq} = E_s(1 - a) + E_c \cdot a \quad (5)$$

Where $a = A_c/A_{total}$ is the area replacement ratio. The one-dimensional elastic settlement under a uniform stress q acting over a layer of thickness H can then be estimated as:

$$s = q.H / E_{eq} \quad (6)$$

These simplified formulations have been widely adopted in practice and in parametric studies of stone columns, and they provide a useful framework for interpreting the E_{50} experimental results obtained in this study. More advanced analyses using three-dimensional finite element or finite difference methods may be required when group effects, complex stratification, or significant lateral deformations are involved.

2.3. Unit cell concept, idealization, and experimental setup

To simulate the behavior of a single stone column embedded in an infinite grid system, the unit-cell concept was adopted. This approach assumes that a large group of stone columns behaves like an infinite array, in which each column and its tributary soil act as axisymmetric units subjected to identical loading and boundary conditions. Within such an arrangement, the settlement of the soil and stone column is approximately equal, and the loading on the top of the unit cell can be idealized as a rigid plate condition. This model is analogous to a one-dimensional consolidation test, in which loading occurs along the K_0 stress path and bearing capacity failure is typically not observed.

Previous investigations, including large-scale tests conducted at the Building Research Establishment in England, demonstrated that the response of unit-cell models closely resembles consolidation behavior without distinct failure (Priebe, 1995). In practical applications, however, stone column groups are finite in size, and the perfect unit-cell conditions of infinite boundary rigidity are rarely achieved due to lateral spreading and bulging. Existing analytical methods for settlement estimation are broadly classified into (i) simplified approaches that employ idealized assumptions, and (ii) advanced methods based on elasticity and plasticity theories, such as the finite element method (FEM), which incorporate realistic material and boundary conditions. The unit cell framework provides the theoretical foundation for several widely used settlement prediction methods, including those proposed by Han (2002) and Priebe as well as FEM-based analyses that assume an infinitely wide loaded area reinforced with stone columns of constant diameter and spacing.

2.4. Laboratory unit cell model and test setup

The experimental investigation was conducted using a physical model designed to replicate the idealized unit cell condition (Fig. 5). The test tank consisted of a composite cylindrical container with an internal diameter of 380 mm, height of 1,000 mm, and wall thickness of 10 mm, providing sufficient rigidity to prevent lateral deformation during loading. The loading

system (Fig. 6) comprised a rigid loading frame equipped with a proving ring for load measurement and a Linear Variable Differential Transformer (LVDT) for precise settlement monitoring.

The loading procedure was as follows:

The load was applied incrementally through a circular steel plate positioned at the top of the column.

Each load increment was maintained for approximately 2.5 minutes to ensure stabilization before the next increment.

The test continued until the total settlement reached 40 mm, corresponding to approximately 100% of the column diameter.

Load-settlement data were continuously recorded throughout the test to establish stress-strain relationships for performance evaluation.

For reference and comparison, identical loading tests were also performed on untreated soft clay beds, allowing direct quantification of the improvement achieved by the geogrid-reinforced stone columns.

2.5. Experimental setup and procedure

2.5.1. Material Properties and Sample Preparation

Soil properties: The experimental soil used in this study is soft clayey soil in a plastic to liquid state, collected from a depth of 3.0 meters at the Quy Nuong Garden Project site, No. 4 Hung Nguyen Street, Thuong Tin Town, Thuong Tin District, Hanoi, Vietnam (Ho Thuong Tin area). The soil was subjected to a series of laboratory tests to determine its physical properties and classification, following ASTM standards.

Grain size distribution and Atterberg limits were determined according to ASTM D422 (2007) and ASTM D4318 (2017), respectively. Based on the test results, the soil is classified as clayey silt to silty clay, with relatively high plasticity (Table 1).

Table 1. Summarizes of soil properties of the soft soil used in the model tests

Property	Symbol	Unit	Value
Natural water content	*w*	%	46.7
Clay fraction (<0.002 mm)	–	%	26.1
Liquid limit	*LL*	%	50.1
Plastic limit	*PL*	%	35.4
Consistency index	*Ic*	–	0.78
Wet unit weight	*γ*	kN/m³	16.6
Specific gravity of solids	*Gs*	kN/m³	26.8
Void ratio	*e*	–	1.313

Experiments with three soil conditions were controlled by varying the amount of water added. For each soil condition, the water content and undrained shear strength (c_u) were determined using a vane shear test, specifically (Fig. 2):

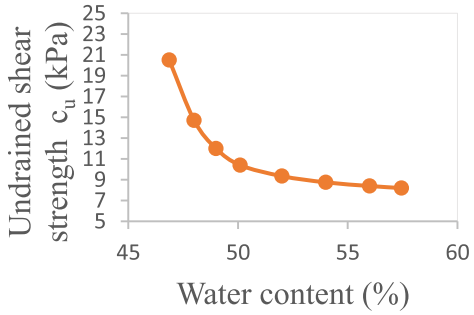

Figure 2. Relationship between unconfined shear strength and soil moisture content

Stone properties: The stone column material used in this study was locally quarried limestone, mechanically crushed and graded. The column material was scaled down to 1/20 of the prototype size for model testing, corresponding to aggregate sizes of approximately 1–4 mm, based on a representative full-scale range of 20–75 mm commonly used in practice.

The gradation of the stone material was carefully selected to:

- Ensure proper compaction and interlocking within the column;
- Limit the fine fraction (< 0.075 mm) to less than 5%, as recommended by Barksdale and Bachus (1983);
- Falls within typical grain-size specifications used in stone-column research.

The particle-size distribution curve of the crushed stone is shown in Fig. 3, confirming compliance with these requirements. The material exhibits a well-graded distribution, favoring load transfer and lateral confinement.

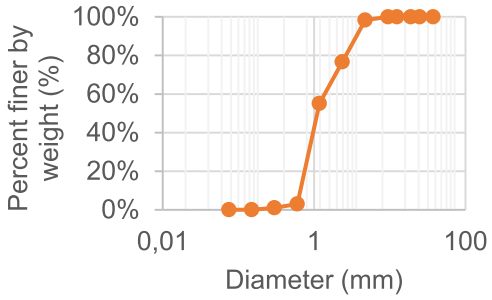

Figure 3. Grain size distribution curve of the aggregate materials used for the stone column

Geogrid properties: In this study, the geogrid used has a maximum tensile strength of 200 kN/m. It is a uniaxial geogrid made from polyester with a polyethylene coating that enhances corrosion, chemical, and impact resistance. Figure 4 shows the results of the geogrid pull-out test, and Table 2 summarizes the properties of the tested geogrids, which were used in the experimental model.

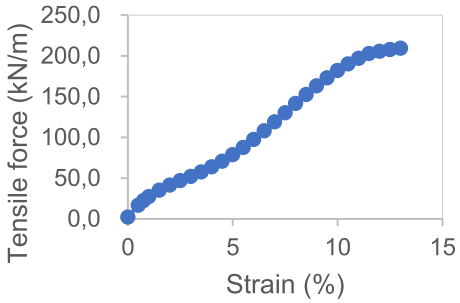

Figure 4. Tensile force-strain relationship of the geogrid

Table 2. Geogrid test results (Tested according to ASTM D6637)

Parameter	Equipment	Unit	Average Value
Tensile strength at roll direction break	X500-100	kN/m	209.4
Elongation at roll direction break	X500-100	%	12
Tensile strength at 2% elongation in roll	X500-100	kN/m	41.4
Tensile strength at 5% elongation in roll	X500-100	kN/m	78.7
Tensile strength in the transverse direction breaks	X500-100	kN/m	105.7
Elongation in the transverse direction breaks	-	%	12

The test setup

The model tests were carried out in a test tank made of composite pipe with dimensions d = 380 mm, h = 1000 mm, and a thickness of 10 mm, as shown in Fig. 5. The tank was sufficiently rigid and showed no lateral deformation. The Loading Frame (Fig. 6) shows the details of the complete setup, which consists mainly of a composite pipe, a loading frame, dial gauges, and accessories.

Figure 5. Test tank made of composite pipe

Figure 6. Loading frame system for single stone column

2.5.2. Model preparation and testing

Preparation of soil: Before preparing the soil bed, a correlation between soil water content and undrained shear strength was established. This correlation ensures that the required shear strength is maintained for each model. The shear strength was determined using the Swedish fall cone penetrometer. Subsequently, the soil bed was prepared through the following steps:

(i) The natural soil was first broken down into small pieces using a hammer, then air-dried for 24 hours; additional crushing was done using a crushing machine.

(ii) The air-dried soil was then divided into batches of 10 kg each.

(iii) Each batch was gradually and thoroughly mixed with an adequate amount of water to achieve a water content within the range of approximately 24–35%.

(iv) After mixing, the soil was placed in layers inside a steel container, with each layer compacted using a specialized tamping hammer of dimensions 50 mm. The thickness of each compacted layer was around 50 mm (Fattah et al., 2011). This layering and compaction process was repeated until the desired total thickness of the soil bed was reached.

(v) Once the soil bed was fully prepared, it was tightly covered with nylon sheets and allowed to cure for four days.

Preparation of stone columns: After completing the soil curing period in the experimental model, the stone column was processed according to the following process:

(i) The soil bed was first leveled.

(ii) The locations where the stone columns were to be installed were accurately marked relative to the loading frame. A hollow PVC tube with an external diameter of 44 mm and a thickness of 2 mm was coated with petroleum jelly and inserted vertically to the specified depths. Additional details for both fully and partially penetrated columns are illustrated in Fig. 7. During extraction, the tube was carefully withdrawn with a twisting motion to minimize disturbance.

(iii) The soil inside the tube was removed, and samples were collected from different depths to determine water content.

(iv) Crushed stone was layered into the prepared hole, with each layer gently compacted using a 30 mm diameter tamping rod. The unit weight of the compacted crushed material stone was recorded as 18.3 kN/m^3. A single stone column with a diameter d = 40 mm and a length L = 600 mm, which corresponds to the thickness of the soft soil layer.

Figure 7. Steps to create a single stone column in the experimental model

2.5.3. Load tests on stone columns

The model tests were executed following the testing program outlined below (Fig. 8), suitable for (Gu et al., 2022):

(i) The proving rings used in the tests were calibrated by applying a range of known static loads and recording the corresponding dial gauge readings. This calibration process was repeated multiple times to improve accuracy.

(ii) The center of the loading plate is aligned with the center of the loading jack.

(iii) A test ring, with an accuracy of 0.01 mm per division, is installed to measure the total load applied to the stone column independently. The Linear Variable Differential Transformer (LVDT) measures the settlement of the stone column.

(iv) The load is applied stepwise through a loading plate.

(v) During each load increase, readings from the settlement gauge linked to the test ring are recorded.

(vi) After each load increase, readings from the settlement gauge are recorded.

(vii) Each load increase is maintained for 2.5 minutes.

(viii) The load increase continues until the total settlement reaches 40 mm, equivalent to 100% of the stone column diameter.

(ix) For comparison, similar load tests were conducted on untreated soil inside the container.

Figure 8. Displacement and load measuring system in a single-stone column experimental model

3. Results and discussion

3.1. Experimental observations and stress-strain behavior

A series of loading tests was performed on single stone columns under two conditions: **Case A** - without geogrid reinforcement, and **Case B** - with a geogrid layer placed on the column head.

The tests aimed to evaluate variations in compressive stress and axial strain under different subsoil conditions. The liquidity index (IL) of the surrounding clay varied from 0.75 to 1.5, representing soil states from plastic to fluid consistency.

Figure 9 illustrates the relationship between axial stress (σ) and relative strain (ε) of the stone column in the case of not using a geogrid (Case A), with the foundation soil exhibiting different liquidity indices. (IL = 0.78; 1.0; and 1.5). The results show that the load-bearing capacity of stone columns decreases significantly with increasing IL, especially without geogrid reinforcement.

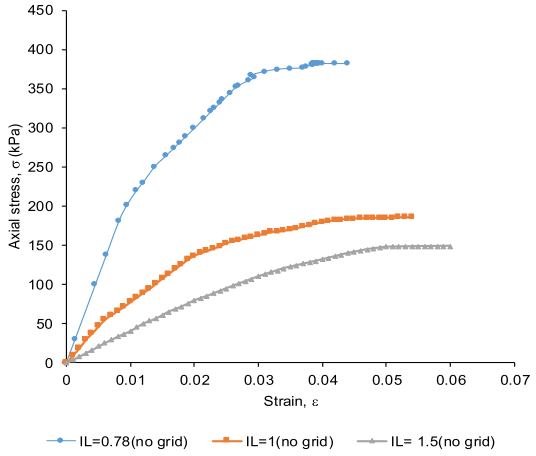

Figure 9. Axial stress (σ) and strain (ε) of the stone column in the case of not using a geogrid

Specifically, at IL = 0.78, the σ–ε curve exhibits a steep slope in the initial stage and reaches a peak stress of approximately 378 kPa, indicating that the column-soil system still exhibits good load and deformation resistance. When IL increases to 1.0, the peak stress drops to around 187 kPa and then sharply to 148 kPa at IL = 1.5. This decrease corresponds to more than a 60% reduction compared to the IL = 0.78 case, reflecting a significant weakening of the soil foundation in a liquid-like state.

In addition, the curves' shapes and slopes indicate that deformation decreases progressively with increasing IL. Notably, at IL = 1.5, the stress increases very slowly with ε, reflecting that the soil foundation is almost incapable of effectively supporting the stone column, which rapidly transitions to a large plastic deformation state.

Figure 10 illustrates the relationship between axial stress (σ) and strain (ε) of a stone column reinforced with geogrid under foundation soil conditions with different liquidity index (IL = 0.78; 1.0; and 1.5). The results indicate that the load-bearing capacity of the column-soil system decreases as IL increases, indicating that the soil gradually transitions from a plastic to a liquid state.

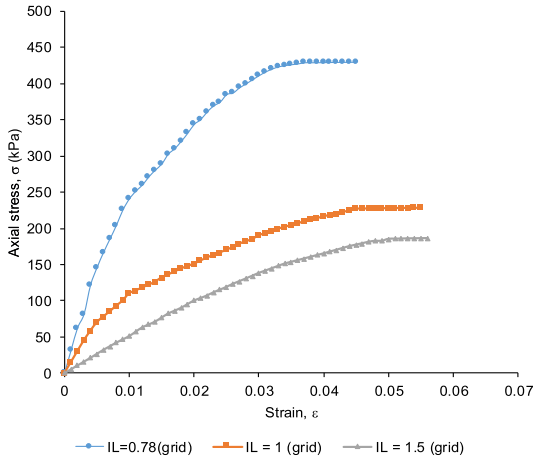

Figure 10. Axial stress (σ) and strain (ε) of the stone column in the case of using a geogrid

Specifically, at IL = 0.78, the stress-strain curve shows a steep slope in the initial stage, reaching a peak stress of approximately 426 kPa. This case represents the highest effectiveness of stone column and geogrid

reinforcement. When IL increases to 1.0, the maximum stress decreases to about 227 kPa and continues to drop to around 188 kPa at IL = 1.5. Simultaneously, the slope of the curve decreases, reflecting the weakening of the stone column's deformation resistance and load-bearing capacity as the foundation soil approaches the liquid limit.

Despite the decrease with increasing IL, all three cases report peak stresses above 180 kPa. This demonstrates the critical role of the geogrid in improving stress distribution and enhancing the overall stability of the stone column reinforcement system, even under soft soil conditions.

3.2. Ultimate bearing capacity and correlation with soil strength

The results of the stone column compression test, conducted in two cases (with and without geogrid), under different soil condition indices (IL = 0.78, 1.0, and 1.5), show a clear influence of soil condition on the stone column's bearing capacity. The correlation between the ultimate bearing capacity of a stone column (qult) and undrained shear strength is compared with that reported by Barksdale et al. (1983) and Han and Ye (Fig. 11).

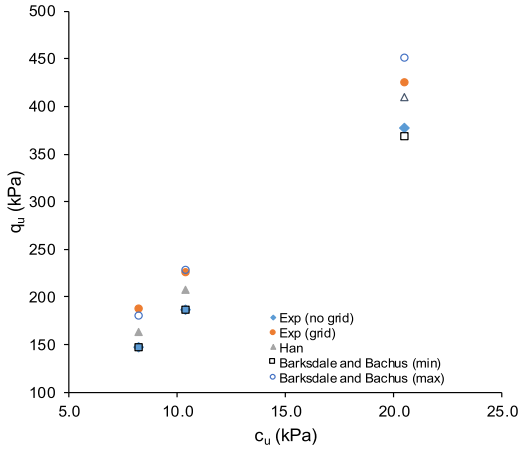

Figure 11. The correlation between the ultimate bearing capacity of the stone column (q_{ult}) and the undrained shear strength

Figure 11 illustrates the relationship between the undrained shear strength of the soft clay (c_u) and the ultimate bearing capacity (q_{ult}) of the stone column under two different conditions: with and without geogrid reinforcement. The experimental data are compared with results from previous studies, including Han and Ye (2001), and the lower and upper bounds proposed by Barksdale and Bachus (1983).

It can be observed that the ultimate bearing capacity of the stone column increases significantly with increasing c_u in all cases. For the same c_u, the use of geogrid consistently results in higher q_{ult} compared to the unreinforced case. For example, at c_u = 10 kPa, the inclusion of a geogrid increased the bearing capacity from approximately 180 kPa (Exp no grid) to 220 kPa (Exp grid), representing an enhancement of about 22%. This improvement can be attributed to the lateral confinement provided by the geogrid, which enhances load transfer and reduces bulging of the stone column.

When compared with the empirical upper and lower bounds proposed by Barksdale and Bachus (1983), the experimental results for the geogrid-reinforced columns fall within both envelopes, indicating good agreement. Notably, the upper bound of Barksdale and Bachus slightly overestimates the observed capacities at higher c_u values, such as 20 kPa. Similarly, Han and Ye's results (2001) are close to the experimental values, particularly in the grid-reinforced condition, suggesting consistency with the behavior predicted in previous literature.

These findings confirm the beneficial role of geosynthetic reinforcement in improving stone column performance, especially in soft soils with low undrained shear strength. Additionally, the results reinforce the importance of considering geogrid reinforcement in analytical and numerical

models used for design, as it provides not only increased strength but also improved stability under load.

These trends are consistent with previous experimental and numerical studies on geosynthetic-reinforced and encased stone columns, which also reported a strong dependency of ultimate capacity on undrained shear strength and a beneficial effect of lateral confinement on limiting bulging and enhancing load transfer. The improvement ratio of about 20–25% in ultimate bearing capacity observed in this study for head-reinforced columns is slightly lower than typical values reported for fully encased systems, which is reasonable given that only local reinforcement at the column head is provided here. Nevertheless, recent experimental and numerical investigations on fully or dual-layer geosynthetic-encased stone columns in soft clays have shown comparable gains in bearing capacity, typically on the order of 15–30% when optimized encasement stiffness and length are adopted, indicating that the performance improvements measured in the present study fall within the range of current research findings. This suggests that head-reinforced geogrid layers can still offer meaningful performance gains while using less geosynthetic material, and may therefore represent a competitive alternative in situations where complete encasement is technically difficult or uneconomical.

3.3. Variation of elastic modulus with soil consistency

Figure 12 presents the analysis results of the elastic modulus E_{50} of a stone column calculated using Equation (1), based on loading tests conducted on a stone column for Case A (without geogrid reinforcement) and Case B (with geogrid reinforcement). For the same soil type, the elastic modulus E_{50} of the stone column with a geogrid layer was significantly higher than that without geogrid reinforcement (Fig. 12a, 12b, and 12c). In addition, the elastic modulus of the stone column decreased as the soil liquidity index (IL) increased, confirming a strong dependence of composite stiffness on the surrounding soil consistency (Fig. 12d).

At IL = 0.78, the reinforced stone column exhibited a higher initial stiffness and peak axial stress compared to the unreinforced column. The E_{50} values were 25,000 kPa for the reinforced case and 21,000 kPa for the unreinforced case, indicating an approximate 19% improvement in stiffness due to the inclusion of geogrid. The stress-strain response also showed a steeper initial slope, reflecting enhanced load transfer and confinement, which agrees with the findings of Barksdale and Bachus (Barksdale et al., 1983), who emphasized the crucial role of stone columns in performance.

At IL = 1.0, both reinforced and unreinforced columns exhibited lower stiffness and peak stress than at IL = 0.78. The E_{50} reduced to 11,330 kPa for the geogrid-reinforced case and 9,350 kPa for the unreinforced case, corresponding to an improvement of about 21% with reinforcement. This confirms that the beneficial effect of the geogrid persists even as the soil consistency softens, although the composite system's absolute stiffness decreases. Similar observations were reported by Madhav and Poorooshasb (1988), who noted that reinforcement efficiency decreases as the surrounding soil approaches very soft conditions.

At IL = 1.5 (soft-to-flow state), the reinforcement effect becomes less pronounced in absolute terms. The E_{50} values were 5,080 kPa (grid) and 4,000 kPa (no grid), which corresponds to an improvement of 27%. However, the absolute stiffness values were markedly lower than in the previous cases, indicating that the surrounding soil governs column performance under very soft conditions. The stress-strain curves for both

reinforced and unreinforced cases converge more closely, suggesting that the geogrid's confinement effect is less effective when the soil is in a near-liquid state. This finding is consistent with Han and Ye (Han and Ye, 2001), who demonstrated that geosynthetic reinforcement is most effective when sufficient lateral restraint can be mobilized.

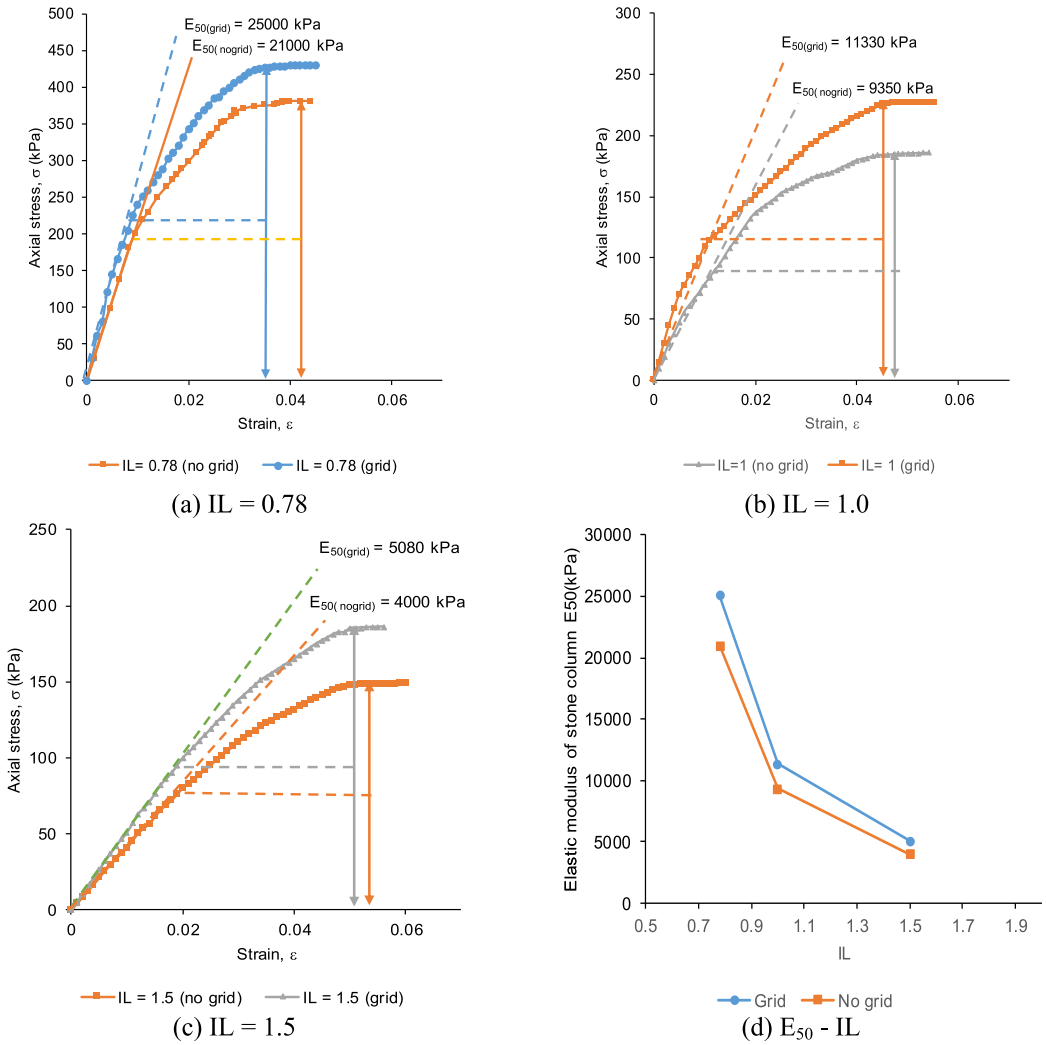

Figure 12. Elastic modulus of the stone column at 50% of the ultimate load

The general trend across all IL values indicates that the modulus of elasticity E_{50} decreases significantly with increasing soil consistency index, highlighting the strong dependence of column performance on the foundation soil's mechanical state. The inclusion of geogrid consistently improves stiffness and load-bearing capacity, but its relative contribution diminishes as the soil transitions toward a flow state. Similar trends were noted by Black et al. (2007) and Gniel and Bouazza (2009), who observed that geosynthetic-encased stone columns offer substantial stiffness gains in firm soils but limited effectiveness in extremely soft conditions.

When viewed in the context of more recent research, the approximately 19–27% stiffness improvements in E_{50} observed in this study are in line with enhancements reported in recent numerical and experimental investigations of geosynthetic-encased stone columns and hybrid reinforced systems in soft soils. Studies on dual-layer and vertically-horizontally encased GESC configurations have shown that appropriate combinations of vertical encasement and horizontal reinforcement can produce significant increases in equivalent composite stiffness and noticeable reductions in settlement under working loads, particularly in soft clay foundations. Within this broader framework, the present results indicate that even localized head reinforcement can deliver stiffness gains of the same order of magnitude as some more material-intensive encasement schemes, while using considerably less geosynthetic material. This reinforces the potential of head-reinforced stone columns as a practical, material-efficient solution for soft clay improvement, especially when full or extended encasement is not feasible due to construction or cost constraints.

4. Conclusions

This experimental study examined the behavior of single stone columns with and without geogrid reinforcement at the column head under varying soft clay conditions characterized by liquidity indices (IL = 0.78, 1.0, and 1.5). Six unit-cell model tests were conducted to evaluate the effects of soil consistency on the ultimate bearing capacity and elastic modulus (E_{50}) of the stone column-soil system. Based on the test results and subsequent analysis, the main conclusions can be summarized as follows:

- The ultimate bearing capacity of the stone column decreases markedly with increasing liquidity index, reflecting the loss of lateral support and increased tendency for bulging in very soft clay. For the same undrained shear strength, the geogrid-reinforced columns consistently exhibited higher capacities than the unreinforced ones, with improvement ratios on the order of 12–25%. These values are consistent with the range of capacity gains reported in recent experimental and numerical studies on geosynthetic-encased stone columns in soft clays, where optimized encasement layouts typically achieve increases of about 15–30% relative to untreated conditions.
- The elastic modulus E_{50} also decreases significantly as IL increases, indicating that both the column and the composite ground system become more deformable in very soft conditions. The presence of a geogrid layer at the column head increased E_{50} by approximately 19–27% compared with the unreinforced configuration, demonstrating a clear stiffness enhancement. These stiffness gains are in line with recent findings for dual-layer and vertically-horizontally encased geosynthetic stone column systems, which likewise report noticeable improvements in equivalent composite stiffness and settlement performance in soft clays. The experimental E_{50} values determined in this study provide valuable data that could be incorporated into predictive frameworks using modern computational approaches such as machine learning models, similar to those developed by Pham et al. (2022) for predicting bearing capacity of deep foundations, thereby enabling more efficient design optimization for geogrid-reinforced stone columns under varying soil conditions.
- The beneficial effect of geogrid reinforcement is most pronounced for moderately soft soils (IL $\leq$ 1.0), where sufficient confinement can be mobilized. In the very soft case (IL = 1.5), the absolute values of E_{50} and bearing capacity are much lower, and the relative improvement due to geogrid, although still present, is more limited. This trend supports the conclusion that the efficiency of geosynthetic reinforcement is strongly governed by the available lateral restraint and the stiffness

contrast between the column material and the surrounding soil, as also emphasized in previous studies on encased stone columns.

Overall, the results indicate that local head reinforcement with a geogrid layer can be a technically material-efficient and straightforward option to enhance the performance of stone columns in soft clay, particularly where full or extended encasement is not feasible due to construction or cost constraints. When viewed alongside recent experimental and numerical research on fully and partially geosynthetic-encased stone columns, the present findings provide complementary evidence that head-reinforced configurations can deliver strength and stiffness improvements of the same order of magnitude as more material-intensive encasement schemes for a relevant range of soft soil conditions. Nevertheless, a detailed cost-benefit analysis and field-scale validation are needed before definitive conclusions on economic efficiency and large-scale applicability can be drawn.

However, the limitation of the present study is the use of a single-column unit-cell model at the laboratory scale and a specific soft clay from the Ho Thuong Tin area, with a limited range of liquidity indices. Group effects, complex stratification, and long-term consolidation behavior were not explicitly addressed. Moreover, only one head reinforcement configuration was investigated, without a direct comparison with fully encased or other partial encasement layouts within the same testing program. Future research should therefore include field tests on column groups, three-dimensional numerical analyses, and extended parametric studies on different reinforcement schemes, combined with economic assessments, to fully evaluate the practical applicability of head-reinforced geogrid stone columns.

Acknowledgements

This research is funded by the University of Transport and Communications (UTC) under grant number T2025-CT-006.

References

Barksdale R.D., Bachus R.C., 1983. Georgia Institute of Technology. School of Civil Engineering. Design and construction of stone columns, I (No. FHWA/RD-83/026;SCEGIT-83-104).

Bergado D.T., Singh N., Sim S.H., Panichayatum B., Sampaco C.L., Balasubramaniam A.S., 1990. Improvement of soft Bangkok clay using vertical geotextile band drains compared with granular piles. Geotextiles and Geomembranes, 9, 203–231. https://doi.org/10.1016/0266-1144(90)90054-G.

Black J., Sivakumar V., McKinley J.D., 2007a. Performance of clay samples reinforced with vertical granular columns. Can. Geotech. J., 44, 89–95. https://doi.org/10.1139/t06-081.

Black J., Sivakumar V., McKinley J.D., 2007b. Performance of clay samples reinforced with vertical granular columns. Can. Geotech. J., 44, 89–95. https://doi.org/10.1139/t06-081.

Bowles J.E., 1996. Foundation analysis and design, 5th ed. ed. McGraw-Hill, New York.

Cheng Y., Mo H., Gu M., 2023. Numerical Analysis on the Behavior of Floating Geogrid-Encased Stone Column Improved Foundation. Buildings, 13, 1609. https://doi.org/10.3390/buildings13071609.

Dash S., Bora M., 2013. Improved performance of soft clay foundations using stone columns and geocell-sand mattress. Geotextiles and Geomembranes, 41, 26–35. https://doi.org/10.1016/j.geotexmem.2013.09.001.

Dheerendra Babu M.R., Nayak S., Shivashankar R., 2013. A Critical Review of Construction, Analysis and Behaviour of Stone Columns. Geotech Geol Eng., 31, 1–22. https://doi.org/10.1007/s10706-012-9555-9.

Fatahi B., Basack S., Premananda S., Khabbaz H., 2012. Settlement prediction and back analysis of Young's modulus and dilation angle of stone columns. AJCE, 10. https://doi.org/10.7158/C11-700.2012.10.1

Fattah M., Shlash K., Jafar Al-Waily M., 2011. Stress Concentration Ratio of Model Stone Columns in Soft Clays. Geotechnical Testing Journal, 34. https://doi.org/10.1520/GTJ103060.

Fattah M.Y., Al-Neami M.A., Shamel Al-Suhaily A., 2017. Estimation of bearing capacity of floating group of stone columns. Engineering Science and Technology, an International Journal, 20, 1166–1172. https://doi.org/10.1016/j.jestch.2017.03.005.

Gniel J., Bouazza A., 2009. Improvement of soft soils

using geogrid encased stone columns. Geotextiles and Geomembranes, 27, 167–175. https://doi.org/10.1016/j.geotexmem.2008.11.001.

Gu M., Mo H., Qiu J., Yuan J., Xia Q., 2022. Behavior of floating stone columns reinforced with geogrid encasement in model tests. Frontiers in Materials, 9, 980851. https://doi.org/10.3389/fmats.2022.980851.

Han J., 2002. A Theoretical Solution for Consolidation Rates of Stone Column-Reinforced Foundations Accounting for Smear and Well Resistance Effects. International Journal of Geomechanics, 2. https://doi.org/10.1061/(ASCE)1532-3641(2002)2:2(135).

Han J., Ye S.-L., 2001. Simplified Method for Consolidation Rate of Stone Column Reinforced Foundations. Journal of Geotechnical and Geoenvironmental Engineering, 127, 597–603. https://doi.org/10.1061/(ASCE)1090-0241(2001)127:7(597).

Hardin B.O., Black W.L., 1968. Vibration Modulus of Normally Consolidated Clay. Journal of the Soil Mechanics and Foundations Division 94, 353–369. https://doi.org/10.1061/JSFEAQ.0001100.

Hasan M., Samadhiya N., 2016. Experimental and Numerical Analysis of Geosynthetic-Reinforced Floating Granular Piles in Soft Clays. International Journal of Geosynthetics and Ground Engineering, 2. https://doi.org/10.1007/s40891-016-0062-6.

Hughes J.M.O., Withers N.J., Greenwood D.A., 1975. A field trial of the reinforcing effect of a stone column in soil. Geotechnique, 25, 31–44. https://doi.org/10.1680/geot.1975.25.1.31.

Indraratna B., Basack S., Rujikiatkamjorn C., 2013. Numerical Solution of Stone Column-Improved Soft Soil Considering Arching, Clogging, and Smear Effects. Journal of Geotechnical and Geoenvironmental Engineering, 139, 377–394. https://doi.org/10.1061/(ASCE)GT.1943-5606.0000789

Kahyaoğlu M.R., Doğan T., 2022. Numerical Study on the Deformation Behavior of Geosynthetic-Encased Stone Columns Supporting Embankments. Teknik Dergi, 33, 12617–12634. https://doi.org/10.18400/tekderg.949826

Ling Z., Ze-yu X.U., Ming-hua Z., 2020. Experimental research on behaviors of geogrid-encased stone column-improved composite foundation under cyclic loads. Chinese Journal of Geotechnical Engineering, 42(12), 2198–2205. https://doi.org/10.11779/CJGE202012005.

Madhav M.R., Poorooshasb H.B., 1988. A new model for geosynthetic reinforced soil. Computers and Geotechnics, 6, 277–290. https://doi.org/10.1016/0266-352X(88)90070-5.

McCabe B., Egan D., Nimmons G., 2009. A review of field performance of stone columns in soft soils. Proceedings of The Institution of Civil Engineers-geotechnical Engineering - Proc Inst Civil Eng-Geotech E., 162, 323–334. https://doi.org/10.1680/geng.2009.162.6.323.

Miranda M., Da Costa A., 2016. Laboratory analysis of encased stone columns. Geotextiles and Geomembranes, 44, 269–277. https://doi.org/10.1016/j.geotexmem.2015.12.001.

Mitchell J.K., 1981. State of the art-soil improvement, in: Proceedings of the 10th ICSMFE, 509–565.

Muzammil S., Varghese R., Joseph J., 2018. Numerical Simulation of the Response of Geosynthetic Encased Stone Columns Under Oil Storage Tank. International Journal of Geosynthetics and Ground Engineering, 4. https://doi.org/10.1007/s40891-017-0122-6.

Ng K.S., Tan S., 2015. Settlement Prediction of Stone Column Group. Int. J. of Geosynth. and Ground Eng., 1, 1–33. https://doi.org/10.1007/s40891-015-0034-2.

Pham T.B., Dam D.N., Bui T.Q.A., Nguyen D.M., Vu T.T., 2022. Estimation of load-bearing capacity of bored piles using machine learning models. Vietnam Journal of Earth Sciences, 44(4), 470–480. https://doi.org/10.15625/2615-9783/17177.

Priebe H.J., 1995. The design of vibro replacement. Ground Engineering.

Singh, I., Sahu, A., 2019. A Review on Stone Columns used for Ground Improvement of Soft Soil. https://doi.org/10.11159/icgre19.132.

Srijan, Ashok Kumar Gupta, 2023. "Horizontally Layered and Vertically Encased Geosynthetic Reinforced Stone Column: An Experimental Analysis" Applied Sciences, 13(15), 8660. https://doi.org/10.3390/app13158660.

Yoo C., Lee D., 2012. Performance of geogrid-encased stone columns in soft ground: Full-scale load tests. Geosynthetics International, 19, 480–490. https://doi.org/10.1680/gein.12.00033.

Zhang X., Liu H., Wang L., 2024. Field tests on partially geotextile encased stone column-supported soft clay foundations. Geotextiles and Geomembranes, 53, 1–15. https://10.1016/j.geotexmem.2023.09.005.